We are IntechOpen,
the world's leading publisher of
Open Access books
Built by scientists, for scientists

6,900
Open access books available

186,000
International authors and editors

200M
Downloads

154
Countries delivered to

Our authors are among the

TOP 1%
most cited scientists

12.2%
Contributors from top 500 universities

BOOK CITATION INDEX
CLARIVATE ANALYTICS
INDEXED

WEB OF SCIENCE™

Selection of our books indexed in the Book Citation Index
in Web of Science™ Core Collection (BKCI)

Interested in publishing with us?
Contact book.department@intechopen.com

Numbers displayed above are based on latest data collected.
For more information visit www.intechopen.com

Folding and Binding Properties of Human Complement Receptor Type 1 Extracellular Domain

Noriyuki Ishii

Additional information is available at the end of the chapter

Abstract

Complement receptor type 1 (CR1 or CD35) is a peripheral glycosylated membrane protein that regulates the complement activation in the control of immune responses. The author would like to overview the folding and binding properties of the soluble form of CR1, so-called as sCR1, introducing our development of the high-yield overexpression and purification methods as well as the investigation to its molecular structure. Although sCR1 prepared through our method showed the highest binding affinity against C3b, it is quite difficult to be crystallized for X-ray structure analysis. In spite of many attempts, only microcrystals have been obtained so far. Considering the usefulness to understand factors within the difficulty, the primary sequence of sCR1 has been reexamined from the viewpoints both of secondary structure predictions and recent findings of intrinsically disordered proteins (IDPs) or natively unfolded proteins (NUPs). As an example, the theoretically predicted structure of a short consensus repeat (SCR) of a binding domain, SCR-15–17 in sCR1 is compared with the reported solution structure by NMR. The discussion is extended to protein structure studies with proteins containing ID regions, which are unfolded state without taking uniformly decided structures.

Keywords: complement receptor type1, CR1, sCR1, innate immunity, dissociation constant, binding affinity, overexpression, molecular structure, secondary structure prediction, crystallization

1. Introduction

Many cellular proteins are believed to fold autonomously to a certain specific three-dimensional structures in order to realize their unique biologically important functions [1, 2]. In the field of protein structural chemistry or structural biology, protein crystallography is fraught with challenge,

whereby various kinds of proteins are known to be difficult to be crystallized. The difficulty may be caused either by polymorphic conformations that the protein takes or movement of regions participating in the contact between molecules in a crystal field [3, 4].

On the other hand, wholly or partly unstructured proteins *in vivo* have been known for a long time and have been recently reevaluated and designated as intrinsically disordered proteins (IDPs) or natively unfolded proteins (NUPs) [5, 6]. It has been revealed that a large number of proteins contain at least a region that does not fold into uniformly converged sophisticated three-dimensional structures. Those regions are sometimes called random coils, which usually indicate globular proteins adopting an unfolded state. It is also not so rare for regions to form chain-like conformations as long as several hundred residues. Since the first review by Wright and Dyson [7], analyses by NMR studies and followed by computational analyses have revealed the importance of IDPs or NUPs in protein structural biochemistry. According to the recent computational survey of primary sequences, it is predicted that the total number of NUPs is approximately one-third of eukaryotic proteins [8].

From the viewpoint of studying functions of proteins, how to recognize and distinguish between self and non-self is still reminded mysterious. Recently, it has become apparent that extracellular membrane vesicles such as exosomes, released from cells are also involved in information transmission between cells in the immune system as well as cancer metastasis [9–12]. In this chapter, the author would like to limit the subject protein to a complement regulatory peripheral membrane protein of innate immunity. Immune adherence was first described at the beginning of the twentieth century and was rediscovered in the 1950s [13, 14]. The binding of serum-exposed particles to blood cells, which is a fundamental step for initiating and promoting the destruction of invasion microbes and for activating an adaptive immune system. This interaction is dependent on the coating of the antigenic particle with the complement, and the recognition by a factor on the erythrocyte surface, namely the immune adherence receptor [15, 16]. Recently, not only infectious microorganisms such as Salmonella, pathogenic *Escherichia coli*, influenza virus and so forth but also causative substances of pollinosis and allergies are widely known as a trigger, further similar causes are increasing including artificial nanoparticles. The complement system, comprised of over 35 protein components present in the plasma or bound to cell surfaces, forms an integral part of the early innate immune response. Three major complement cascades such as classical-, alternative-, and mannose-binding lectin pathways are known to activate the complement pathway and for excluding harmful invaders.

Complement receptor type 1 (CR1 or CD35) is a glyco-membrane protein that plays a role as a regulator of complement activation in the control of immune responses through its binding to C3b/C4b-opsonized foreign antigens [17]. The existence of allotypes is known to CR1, and the molecular mass varies from 160 to 250 kDa depending on its types. The extracellular portion of the most common allotype has about molecular mass of 220 kDa and is comprised of 30 modules, a series of tandem arranged short consensus repeat (SCR) (**Figure 1**). The sequence of each SCR shows approximately 45% homogeneity on average. The feature to be noted is the existence of four conserved cysteine residues in each SCR, as the first and third, and the second and fourth cysteines from the N terminus are covalently linked through disulfide bonds [17]. Weisman et al. reported a construction of human CR1 plasmid (pBSCR1c/pTCSgpt) by
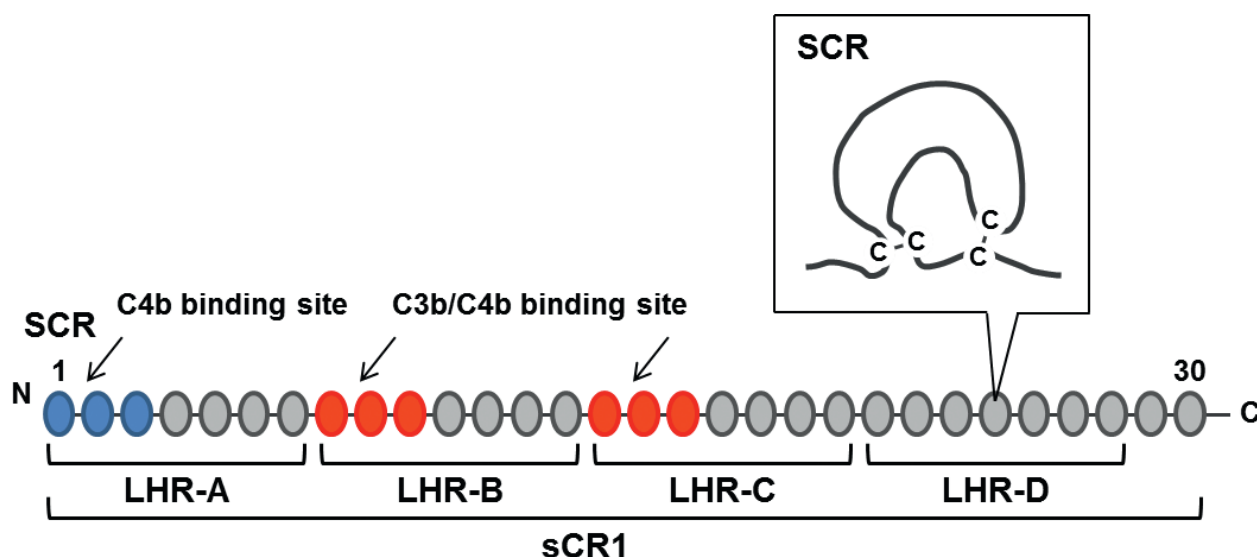
Figure 1. A schematic diagram showing the structural features of human sCR1. The extracellular domain consists of 30 short consensus repeats (SCRs). The amino-terminal 28 SCRs constitute four long homologous repeats (LHRs). The regions of LHR-A through LHR-D are indicated in the brackets. The predicted binding domains to complement proteins C3b, and C4b are indicated, respectively. The inset shows the enlargement of the triple loop structure of SCR with the predicted disulfide bonds.

cloning a soluble CR1 gene to plasmid pTCSgpt, in which a stop codon was inserted before the transmembrane and cytoplasmic domains [18]. As shown in **Figure 1**, the schematic drawing of the predicted structure of human sCR1 shows sCR1 consisting of four long homologous repeats (LHRs) constituted with seven SCRs, which are referred as LHR-A, -B, -C, and -D from N terminus. A binding domain to complement fragment C4b resides near N-terminus in LHR-A, and two domains to C3b reside LHR-B and LHR-C. The C3b binding domains appear to bind C4b but more weakly than C3b.

Although sCR1 may not fall exactly within the category of NUPs (or IDPs) because it has structured domains arranged at intervals tandemly, we think that it is important to consider the analysis of sCR1 from the perspective of NUPs (or IDPs).

2. Materials and methods

2.1. Preparation of human sCR1 from the cultivation with CHO cells

The cell line of Chinese hamster ovary (CHO) (CRL-10052) that carries the human sCR1 gene was purchased from American Type Culture Collection (ATCC) and was cultured under the ATCC's instructions. The human sCR1 was overexpressed using our novel cell culture method comprised of two-stage cell culture of CHO cells expressing sCR1 [19, 20]. The first stage involves cells grow up to 70–80% confluent in the medium with fetal bovine serum (FBS), and during the second stage, the cells produce sCR1 extensively and secrete it in a serum-free medium. For the first stage of cell growth culture, cells were cultivated in a medium containing α-MEM (Sigma-Aldrich Co. LLC., MO) supplemented with 10% FBS (Hyclone Lab. Inc., UT), 60 U/mL penicillin

and 60 μg/mL streptomycin (Pen Strep, Gibco, Life Technologies Corp., CA). Medium used for CHO cell culture was especially chosen, without deoxyribonucleoside and ribonucleoside. For the second stage of protein production, the cells were cultured in a serum-free medium such as ASF104 without albumin (Ajinomoto Co. Inc., Tokyo, Japan) supplemented with 1 μM methotrexate. Cell culture was performed in the incubator with 5% CO_2 at 37°C.

The serum-free medium which contains the secreted human sCR1 was recovered after a filtration (pore size of 0.22 μm). Subsequently, the purification of human sCR1 was performed by affinity column chromatography using HiTrap Heparin HP (GE Healthcare, PA). Briefly, the filtered medium solution was applied to the column that had been pre-equilibrated with 20 mM Tris-HCl buffer (pH 7.5) containing 0.05% CHAPS (Dojindo Molecular Technologies, Inc., Kumamoto, Japan). The column was washed with the equilibration buffer containing 100 mM NaCl, and the bound protein was eluted with 20 mM Tris-HCl buffer (pH 7.5) containing 0.05% CHAPS and 200 mM NaCl. Each eluted fraction sample was examined with sodium dodecyl sulfate polyaclylamide gel electrophoresis (SDS-PAGE) and subsequent Coomassie Brilliant Blue (CBB) staining. Though in most cases, a single or a considerably major band which corresponds to human sCR1 can be observed at this stage, to achieve the buffer exchange concurrently and further examine the purity, the fractions containing sCR1 gathered from the eluents from the heparin column was injected to HPLC gel filtration column chromatography (TSK gel G3000SWxl, Tosoh Corp., Tokyo, Japan). The single peak fraction at around the elution volume of 5.75 ml with a flow rate of 0.5 ml/min was collected as a purified human sCR1 [21]. Complement protein C3b was purchased from Calbiochem Research Biochemicals (EMD Bioscience, Inc., La Jolla, CA), and used after HPLC gel filtration column chromatography (TSK gel G3000SWxl, Tosoh Corp., Tokyo, Japan).

2.2. Characterization of binding affinity of sCR1 for C3b, and suppression effect of cell necrosis by sCR1

In order to investigate the binding affinity of the human sCR1 prepared by our protocol mentioned above, binding assay was performed by the use of a BIACORE X (GE Healthcare UK Ltd., Buckinghamshire, UK) using C3b as an analyte. The measurement was carried out using sCR1 as a ligand, immobilized on a substrate by the amine coupling method, and following the manufacturer's operation manual. In addition, assuming heterogeneous ligand parallel reaction, data analysis was performed by the software, BIAevaluation attached to the device.

The suppression effect of sCR1 on complement activation was examined as follows: a stroma cell derived from mouse skull bone marrow was used for this assay. PA-6 cells were seeded and allowed to grow in the medium containing α-MEM (Sigma-Aldrich Co. LLC., MO) with 10% FBS for 1 day. After three washes with PBS, cells were added with serum-free medium (900 μL of α-MEM) as well as 100 μL of PBS solution containing sCR1 and normal human serum (NHS) at a ratio of 1:9, or 100 μL of PBS solution containing sCR1 and heat-inactivated NHS at a ratio of 1:9. After 1 h incubation at 37°C, the suppression effect on the necrosis of cells was observed with a microscope (Zeiss Axiovert 200 M and Nikon DP50-WMED) following the previous methods [22–24].

2.3. Crystallization trials

Crystallization using thus obtained human sCR1 was carried out with a normal sitting drop vapor diffusion technique in the combination with a random-screening protocol with screen packages such as the Hampton Crystal Screen, Hampton Crystal Screen II (Hampton Research, CA), and Structure Screen 1 and Structure Screen 2 (Molecular Dimensions, Suffolk, UK) after the condensation to the protein concentration of around 3.5 mg/mL by means of centrifugal concentrator (Centri-plus 20, Merck Millipore Corp., MA). The incubation temperature for the crystallization trials was kept at around 23°C [4, 25].

2.4. Secondary structure prediction of human sCR1

The secondary structure predictions of human sCR1 on the basis of its primary sequence were performed by the use of PArallel Protein Information Analysis (PAPIA) system (http://cbrc3.cbrc.jp/papia/), parallel calculation using EnterPrise 4000 with 250 MHz UltraSPARC II 9pu, at the Computational Biology Research Center, AIST [26, 27]. The computing strategies employed were Chou-Fasman algorithm, and the joint prediction method where the protein secondary structure results of five different independent prediction methods were evaluated. In the latter calculation, the most likely secondary structure element for each amino acid sequence region of interest is decided from five independent answers depending on the decision by majority. The five methods incorporated are Qian-Sejnowski, Ptitsyn-Finkelstein, Nisikawa-Ooi, SSthread (prediction of protein secondary structure using threading), and Gibrat-Garinier-Robson methods. They were chosen from different methodologies on the basis of their performance.

3. Results and discussion

3.1. Characterization of sCR1 binding affinity for C3b

The intrinsic state, that is, if the protein is in the original structural state, its activity should be retained. Therefore, it can be considered that the purified protein assumes the same three-dimensional structure as when it is present *in vivo*. The binding affinity of the overproduced and purified human sCR1 for the complement C3b was investigated by biophysical interaction analysis with BIACORE X. The scheme in **Figure 2(a)** shows an outline of the measurement, and **Figure 2(b)** shows one of the typical results of sensorgram. In the light of the manufacture's protocol for data analysis, we have analyzed the data on the assumption of heterogeneous ligand parallel reaction and found that the dissociation constants of sCR prepared according to our production and purification method were $Kd = 3.03 \times 10^{-10}$ M for C3d dimer, and $Kd = 4.59 \times 10^{-9}$ M for C3b monomer, which are higher affinity than any values reported so far [18, 28–32]. It turned out that the binding affinities for C3b of the sCR1 prepared by our developed procedure are remarkably strong. We consider that the reason is due to the rapid and efficient purification method developed by us that can preserve sCR1 in an intact state.
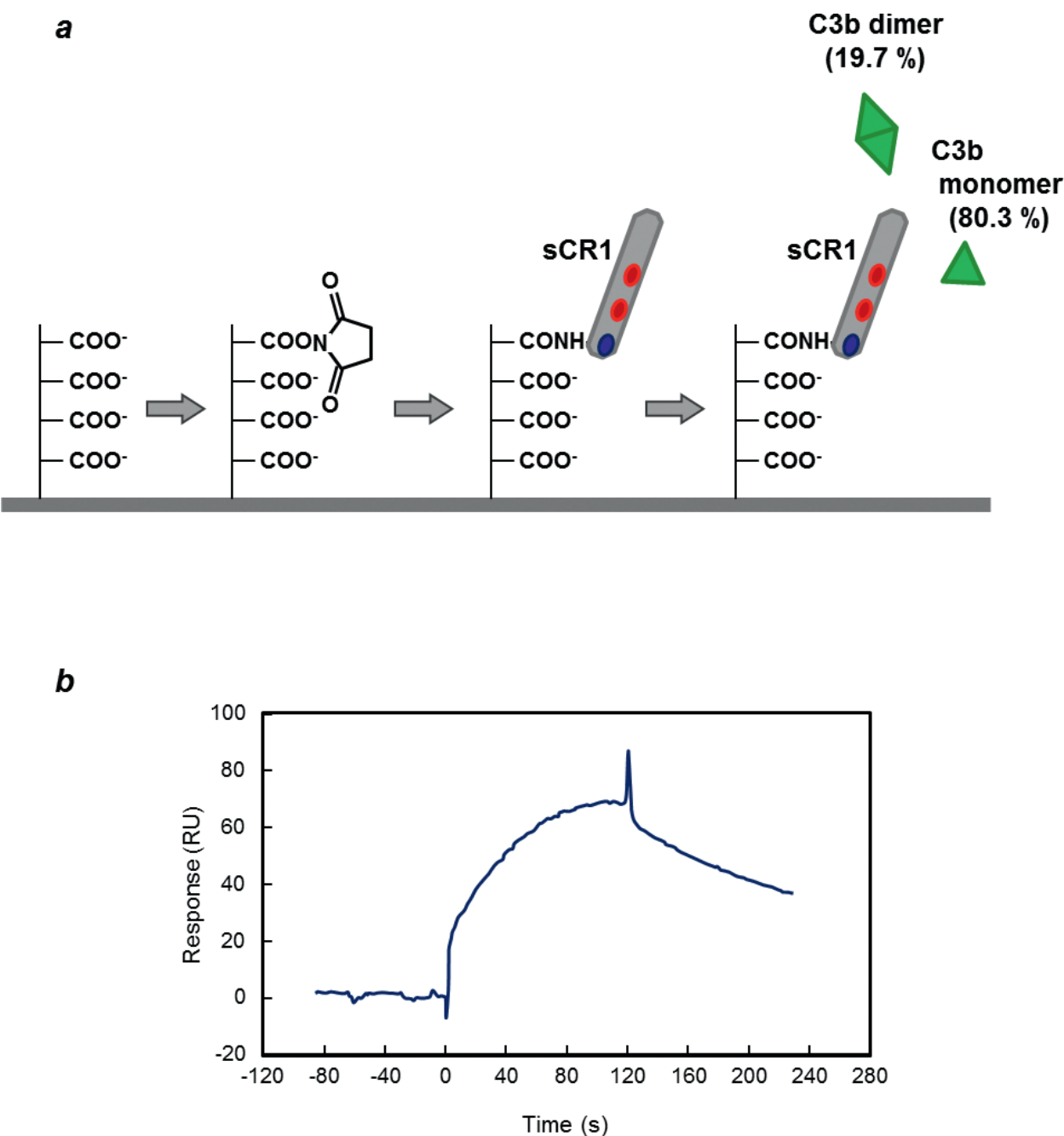
Figure 2. (a) A schematic drawing of the binding assay measurement by BIACORE. In complement C3b solution used as an analyte, monomeric and dimeric forms in C3b are recognized. The existence ratio between C3b monomer and C3b dimer was confirmed on HPLC gel permeation column chromatography. (b) A typical result of sensorgram from the biophysical interaction analysis with BIACORE X.

3.2. Characterization of sCR1 suppression effect of cell necrosis

In order to investigate the suppression effect of sCR1 on complement activation, a stroma cell PA-6 derived from mouse skull bone marrow was used for the assay. Human serum comprises complement proteins C1–C9, which trigger the activation of complement pathways and attack invading target microbes or non-self-cells. The complement pathway ends with the

necrosis of target cells due to the attack by C5b-9 membrane attack complex (MAC) [22, 23]. MAC is an important innate immune effector of the complement terminal pathway that forms cytotoxic pores on the surface of microbes. Similarly to CR1, the conformation in three-dimension of MAC is also unknown. In order to determine whether the purified human sCR1 retains its activity to bind complement C3b and/or C4b and suppresses the necrosis of cells by blocking complement pathway, sCR1 was added to PA-6 cells before the addition of the normal human serum (NHS). The results are shown in **Figure 3**. Cells cultured in medium were used as a control (**Figure 3(a)**), and cells cultured with inactivated NHS show similar results as the control; all cells grew well and maintained their normal morphology (**Figure 3(b)**). This fact implies that the inactivated complements in the serum cannot trigger any complement pathway. However, cells cultured with NHS reveal remarkable necrosis (**Figure 3(c)**). It implies that NHS triggers the activation of complement pathway and MAC attacks the cell membrane and causes cell death. On the other hand, when cells were cultured in the presence of NHS as well as the purified sCR1, cells showed normal morphology without any necrosis although most of cells appeared slim in their shape (**Figure 3(d)**). These results proved that the purified sCR1 has an activity to bind C3b and C4b in NHS and play a role as a blocker to the activation of MAC.
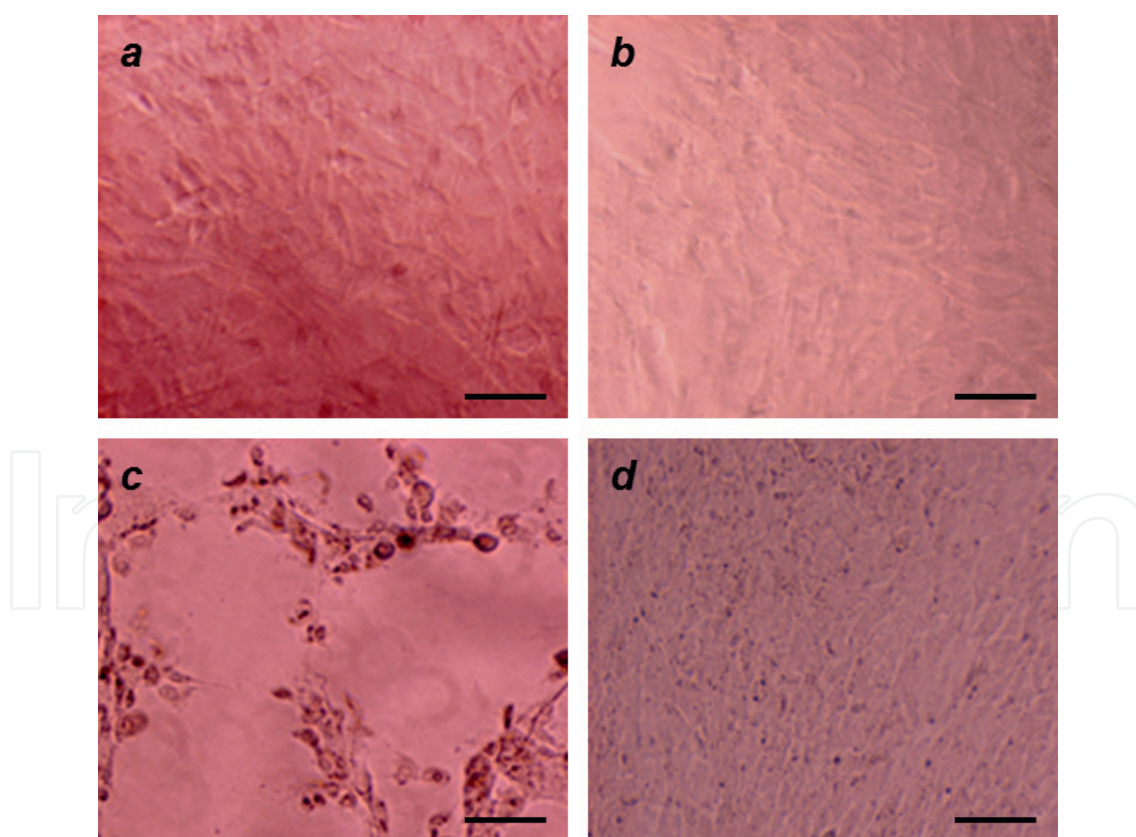
Figure 3. Suppression effect of cell necrosis by sCR1 on stroma cell PA-6. Phase contrast micrographs of PA-6 cells in (a) α-MEM media (control), (b) in the presence of heat inactivated NHS, (c) in the presence of NHS, and (d) in the presence of NHS plus the purified sCR1. Cell necrosis is observed when the formation of membrane attack complex (MAC) located at the complement terminal pathway is not inhibited. The scale bars correspond to 100 μm.

3.3. Crystallization trials

Although we have not yet fully succeeded in obtaining crystals of sCR1 suitable for X-ray crystallographic experiments, the microcrystals have been obtained more than 10 years after the continuous re-innovation of cell culture methods and protein purification strategies. **Figure 4** shows the micrographs of thus obtained microcrystals of sCR1. These crystals are obtained under the conditions where sulfate and polyethylene glycol (PEG) of low polymerization degree were used as precipitants (Kato and Ishii, unpublished data). Those microcrystals diffract X-ray up to several tens of angstrom units, only in a small angle region (data not shown) [33].

Furtado et al. reported the structural model as a partly folded back solution structure of human sCR1 by using a combination of small angle X-ray scattering and analytical ultracentrifugation analyses [34]. They constructed the sCR1 model using a SCR segment as a building block unit. The average model of the consensus SCR domain used was derived from 27 different experimental SCR structural templates and 49 residue consensus SCR sequence from 124 human complement sequences. They connected the SCRs and build the sCR1 model so as to give a better hit to the X-ray solution scattering profiles. Although they emphasize that one out of the five models is the most likely conformation in a free environment, these five models do not seem to overlap three-dimensionally with each other at all. Their solution structure of human sCR1 reported appears not to be rigid at each inter-SCR connection. The realization of structure
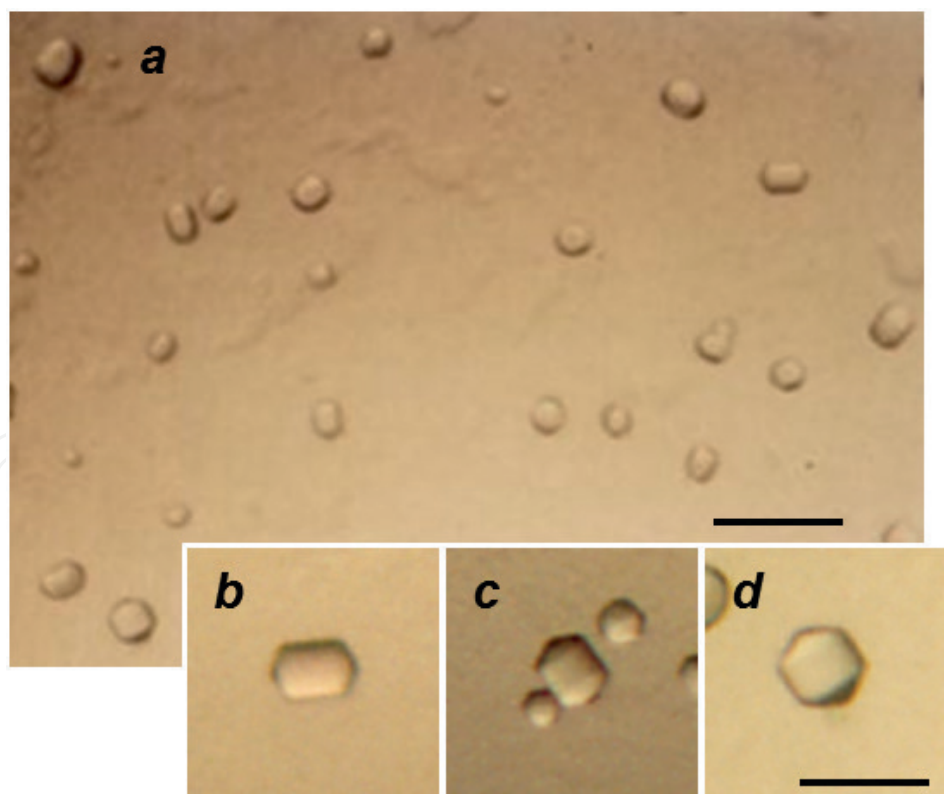

Figure 4. Microcrystals of human sCR1. Approximate dimension of the typical crystals were 29 × 29 × 33 μm. The scale bar in panel (a) corresponds 100 μm, and that for the enlargement, (b)–(d) corresponds 50 μm. Those microcrystals diffract X-ray poorly and spots could be recorded in a small angle range (not shown).

at an atomic resolution of human sCR1 as determined with X-ray crystallography appears very difficult without once forming a rigid complex structure with a complement ligand like C3b, although it is unknown what three-dimensional structured complex would be formed between sCR1 and C3b.

3.4. Secondary structure simulation of human sCR1

To change tactics, it may be useful to compute the secondary structure prediction for the amino acid sequence of a protein whose tertiary structure is not determined [26]. First, we tried the prediction method of Chou-Fasman. The results of secondary prediction for each SCR (from SCR-1 through SCR-30) are exhibited in **Figure 5**. According to the Chou-Fasman method, the content of α-helices is 13.6%, and that of β-strands is 24.9%. Taking a look at the distribution along the sequences of the predicted secondary elements, similarity is recognized between every seventh SCRs. Typically, the homogeneity among the every seventh SCRs between SCR-8–SCR-11 and SCR-15–SCR-18 are remarkable. These regions are considered as a C3b/C4b binding site, thus the conservation in the secondary elements between the above regions is convincible consistent with this observation.

The structural model of the domain from SCR-15 through SCR-17 of human sCR1 was built by Smith et al. [35]. Before building the structural model of the three consecutive SCR domains, they had determined the solution structure of SCR-15–SCR-16, and SCR-16–SCR-17, independently by NMR analyses. As shown in **Figure 6(a)**, the model reveals three complement control modules (SCR-15–17) in extended head-to-tail arrangement with flexibility at the SCR-15–SCR-16, and the SCR-16–SCR-17 junction. **Figure 6(b)** shows the result of quantitative electrostatic calculations. The view orientation is the same as **Figure 6(a)**. In this view angle, the negatively charged surface regions appear to be dominant and appear to be concentrated on the surface of SCR-15, and SCR-17. **Figure 6(c)** is a presentation of SCR-15–16–17 from a different orientation (turned 180°) as shown on the right side of **Figure 6(b)**. The corresponding electrostatics to **Figure 6(c)** is shown in **Figure 6(d)**. At this angle, the positively charged surface regions appear to be connected with one-side surface of SCR-15 through SCR-17. It is said that the positively charged region on SCR-15 is critical for C4b binding, and further, together with basic amino acid residues exposed on the same surface of SCR-16 are requisite for C3b binding [35]. Negatively charged regions are also seen scattered on the surface. The domain architecture and the manner of charged states appear important and may provide clues to the functional aspect of C3b binding.

At this stage, it appears interesting to examine the secondary structure predictions with the model built from the solution structures by NMR analyses. The domain SCR-15–17 (indicated with a box in **Figure 5**) is from a prediction using the Chou-Fasman method (**Figure 5**). α-Helices are not assigned with the solution structure at all (**Figure 6**), though the existence is predicted by the Chou-Fasman method. However, it is interesting that the number of predicted secondary structural elements is almost comparable. We then tried another structure prediction method, that is, the joint prediction method, which had higher precision. **Figure 7** shows the results of secondary prediction for each SCR (from SCR-1 through SCR-30) by the use of the joint prediction method. The content of α-helices is 6.0%, and that of β-strands is

SCR01   42   QCNAPEWLPFARPTNLTDEFEFPIGTYLNYECRPGYSGRPFSIICLKNSVWTGAKDRCRR   101

SCR02   102   KSCRNPPDPVNGMVHVIKGIQFGSQIKYSCTKGYRLIGSSSATCIISGDTVIWDNETPICDR   163

SCR03   164   IPCGLPPTITNGDFISTNRENFHYGSVVTYRCNPGSGGRKVFELVGEPSIYCTSNDDQVGIWSGPAPQCIIP   235

SCR04   236   NKCTPPNVENGILVSDNRSLFSLNEVVEFRCQPGFVMKGPRRVKCQALNKWEPELPSCS   294

SCR05   295   RVCQPPPDVLHAERTQRDKDNFSPGQEVFYSCEPGYDLRGAASMRCTPQGDWSPAAPTCEV   355

SCR06   356   KSCDDFMGQLLNGRVLFPVNLQLGAKVDFVCDEGFQLKGSSASYCVLAGMESLWNSSVPVCEQ   418

SCR07   419   IFCPSPPVIPNGRHTGKPLEVFPFGKTVNYTCDPHPDRGTSFDLIGESTIRCTSDPQGNGVWSSPAPRCGIL   490

SCR08   491   GHCQAPDHFLFAKLKTQTNASDFPIGTSLKYECRPEYYGRPFSITCLDNLVWSSPKDVCKR   551

SCR09   552   KSCKTPPDPVNGMVHVITDIQVGSRINYSCTTGHRLIGHSSAECILSGNAAHWSTKPPICQR   613

SCR10   614   IPCGLPPTIANGDFISTNRENFHYGSVVTYRCNPGSGGRKVFELVGEPSIYCTSNDDQVGIWSGPAPQCIIP   685

SCR11   686   NKCTPPNVENGILVSDNRSLFSLNEVVEFRCQPGFVMKGPRRVKCQALNKWEPELPSCS   744

SCR12   745   RVCQPPPDVLHAERTQRDKDNFSPGQEVFYSCEPGYDLRGAASMRCTPQGDWSPAAPTCEV   805

SCR13   806   KSCDDFMGQLLNGRVLFPVNLQLGAKVDFVCDEGFQLKGSSASYCVLAGMESLWNSSVPVCEQ   868

SCR14   869   IFCPSPPVIPNGRHTGKPLEVFPFGKAVNYTCDPHPDRGTSFDLIGESTIRCTSDPQGNGVWSSPAPRCGIL   940

SCR15   941   GHCQAPDHFLFAKLKTQTNASDFPIGTSLKYECRPEYYGRPFSITCLDNLVWSSPKDVCKR   1001

SCR16   1002   KSCKTPPDPVNGMVHVITDIQVGSRINYSCTTGHRLIGHSSAECILSGNTAHWSTKPPICQR   1063

SCR17   1064   IPCGLPPTIANGDFISTNRENFHYGSVVTYRCNLGSRGRKVFELVGEPSIYCTSNDDQVGIWSGPAPQCIIP   1135

SCR18   1136   NKCTPPNVENGILVSDNRSLFSLNEVVEFRCQPGFVMKGPRRVKCQALNKWEPELPSCS   1194

SCR19   1195   RVCQPPPEILHGEHTPSHQDNFSPGQEVFYSCEPGYDLRGAASLHCTPQGDWSPEAPRCAV   1255

SCR20   1256   KSCDDFLGQLPHGRVLFPLNLQLGAKVSFVCDEGFRLKGSSVSHCVLVGMRSLWNNSVPVCEH   1318

SCR21   1319   IFCPNPPAILNGRHTGTPSGDIPYGKEISYTCDPHPDRGMTFNLIGESTIRCTSDPHGNGVWSSPAPRCELSVRA   1393

SCR22   1394   GHCKTPEQFPFASPTIPINDFEFPVGTSLNYECRPGYFGKMFSISCLENLVWSSVEDNCRR   1454

SCR23   1455   KSCGPPPEPFNGMVHINTDTQFGSTVNYSCNEGFRLIGSPSTTCLVSGNNVTWDKKAPICEI   1516

SCR24   1517   ISCEPPPTISNGDFYSNNRTSFHNGTVVTYQCHTGPDGEQLFELVGERSIYCTSKDDQVGVWSSPPPRCIST   1588

SCR25   1589   NKCTAPEVENAIRVPGNRSFFSLTEIIRFRCQPGFVMVGSHTVQCQTNGRWGPKLPHCS   1647

SCR26   1648   RVCQPPPEILHGEHTLSHQDNFSPGQEVFYSCEPSYDLRGAASLHCTPQGDWSPEAPRCTV   1708

SCR27   1709   KSCDDFLGQLPHGRVLLPLNLQLGAKVSFVCDEGFRLKGRSASHCVLAGMKALWNSSVPVCEQ   1771

SCR28   1772   IFCPNPPAILNGRHTGTPFGDIPYGKEISYACDTHPDRGMTFNLIGESSIRCTSDPQGNGVWSSPAPRCELSVP   1845

SCR29   1846   AACPHPPKIQNGHYIGGHVSLYLPGMTISYICDPGYLLVGKGFIFCTDQGIWSQLDHYCKE   1906

SCR30   1907   VNCSFPLFMNGISKELEMKKVYHYGDYVTLKCEDGYTLEGSPWSQCQADDRWDPPLAKCTSRAHDA   1972
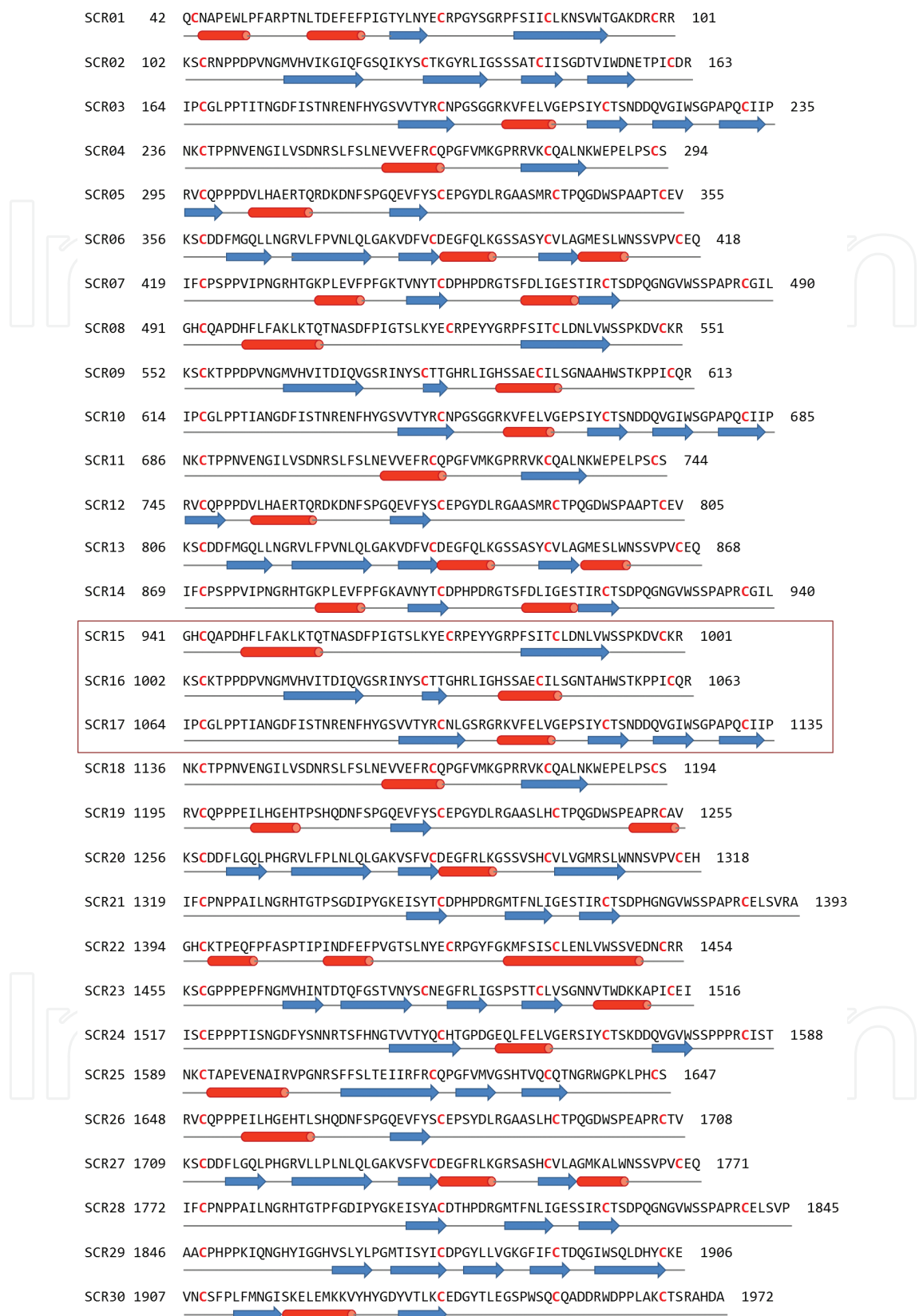
Figure 5. Secondary structure prediction for each SCR (from SCR-1 through SCR-30) in human sCR1 by the use of the Chou-Fasman method. The sequence predicted as α-helix or β-strand is shown with a cylindrical shape or fat arrow, respectively. The predicted sequence except the secondary structural element is a coil shown as a simple rod. The conserved Cys residues in each SCR are highlighted in red. The portion of SCR-15–17 discussed in the text is indicated with a box.
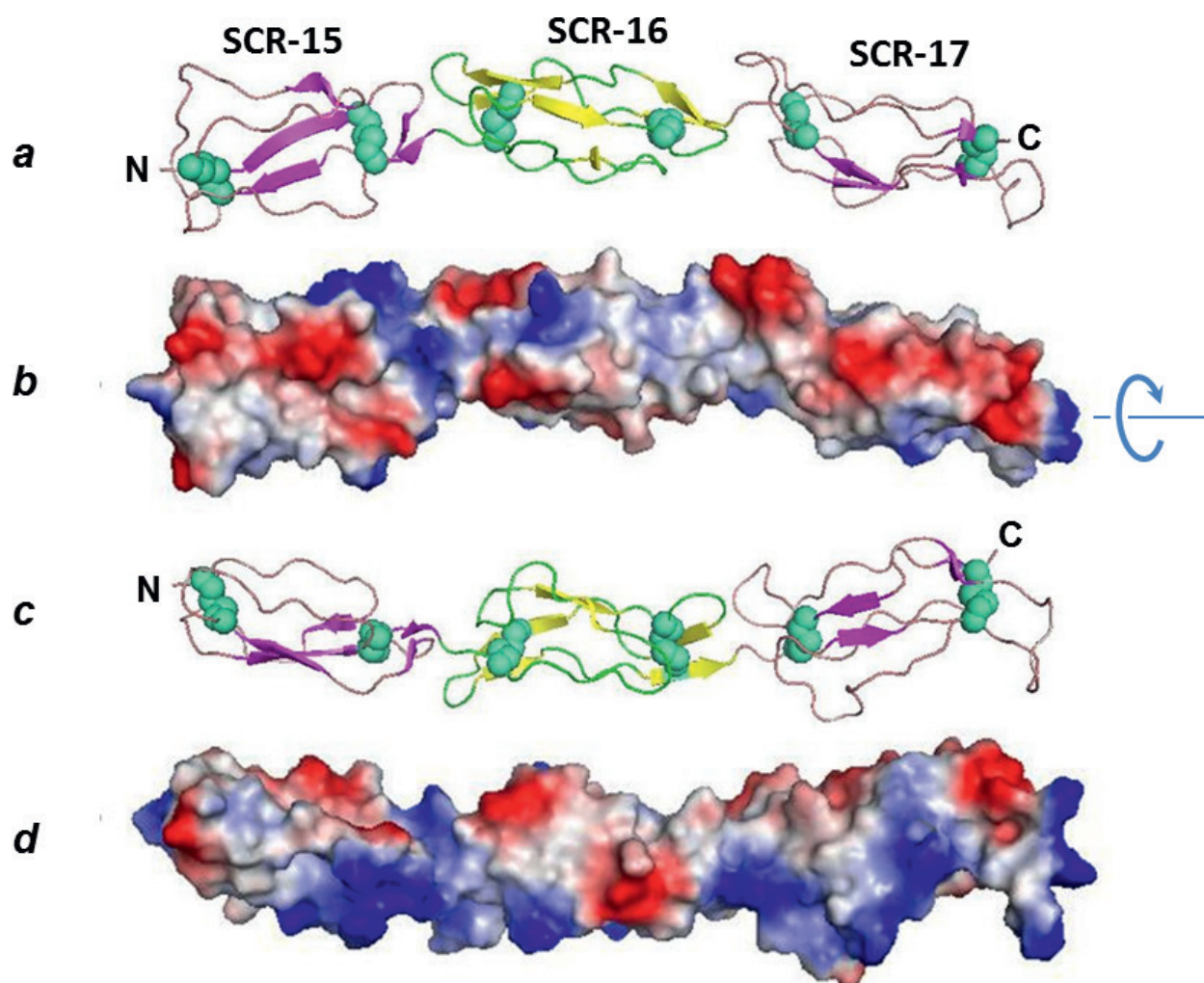
Figure 6. Diagrams of solution structure of domains SCR-15–17 (PDB ID: 1GOP). (a) Cα trace of SCR-15–17 with secondary structural elements (β-strand is indicated with arrow) and disulfide bonds (indicated with spheres). (b) An electrostatic presentation of SCR-15–17; the same view as (a). The protein domains are shown as an electrostatic surface colored blue in the positive regions and red in the negative regions. (c) Cα trace with secondary structural elements and disulfide bonds of SCR-15–17 made to rotate 180° as shown on the right side of (b). (d) An electrostatic presentation of SCR-15–17; the same view as (c). Atomic coordinates were obtained from the RCSB protein data Bank (www.rcsb.org/pdb/home/home.do) and imaged using PyMol (the PyMOL molecular graphics system, version 0.99, DeLano scientific, LLC).

19.3%. The accuracy of results from the joint prediction methods is better than a single method such as Chou-Fasman method, Garinier-Osguthorpe-Robson method, and Lim method [27]. Since the final assessment of whether a certain amino acid sequence forms a secondary structure element is determined by majority rule between five different prediction algorithms, the precision success rate is rather high while the adoption rate as secondary structure elements is low compared to the prediction results by Chou-Fasman method on the whole. Looking at the prediction of SCR-15–17 for example (as indicated with a box in **Figure 7**), all but one predicted secondary elements as β-strands, suggesting that precision rose. The content of α-helices was predicted in the half ratio in comparison with that of β-strands by the Chou-Fasman method, but the prediction of α-helices improved in one-third or less compared with the content of β-strands using the joint method. In the algorithms of the joint prediction method, the most likely secondary structure element for each amino acid sequence region is decided depending
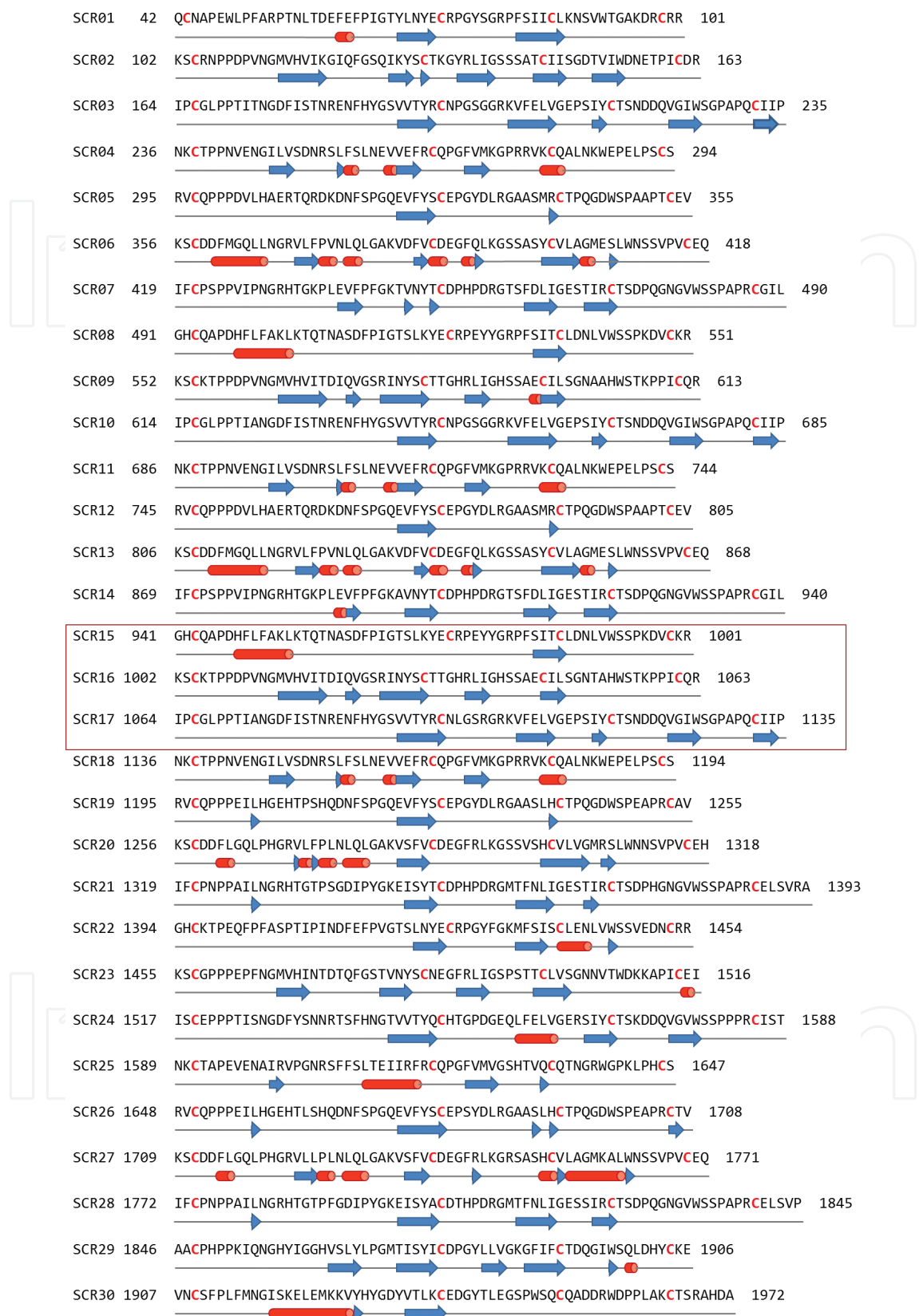
Figure 7. Secondary structure prediction for each SCR (from SCR-1 through SCR-30) in human sCR1 by the use of the joint prediction method. The sequence predicted as α-helix or β-strand is shown with a cylindrical shape or fat arrow, respectively. The predicted sequence except the secondary structural element is a coil shown as a simple rod. The conserved Cys residues in each SCR are highlighted in red. The portion of SCR-15–17 discussed in the text is indicated with a box.

on the decision by majority votes against five independent answers, from Qian-Sejnowski, Ptitsyn-Finkelstein, Nisikawa-Ooi, SSthread, and Gibrat-Garinier-Robson methods. Therefore, a sequence will not be qualified as a secondary structure, either α-helix or β-strand, unless getting an approval from majority solutions. Therefore, the number of region predicted as secondary structured elements as a whole will be decreased, but higher reliability will be expected. The tendencies in the order and distribution of the predicted secondary elements are recognized to be almost the same between every seventh SCRs, especially among the every seventh SCRs between SCR-8–SCR-11 and SCR-15–SCR-18.

3.5. Structural biological aspect of human sCR1

As discussed earlier, determinations of three-dimensional structure of each SCR, and the confidence with subsequent modeling of sCR1 appears severely difficult due to the sequence variation, and the orientation and flexibility of neighboring SCRs with respect to one another appear to easily change considerably, and are thus unpredictable. sCR1 is one of the very difficult targets for structure analysis, but we are convinced that such a goal has some promise once its three-dimensional molecular structure is determined.

Recently, a large number of NUPs have been found, and those appear to be connected with signaling and regulation of gene expression [8]. As exemplified above with sCR1, there are a lot of proteins involved in the immune system whose three-dimensional structure has not yet been revealed by X-ray crystallography. One of the reasons is the difficulties in the preparation of crystals suitable for X-ray diffraction methods probably due to the large flexibility (that may correspond to large values in B factor) of functional and reactive domains and is thus subject to conformational changes. The conceptual importance of NUPs is that various proteins interact with other proteins via intrinsically disordered regions. It means the ID region is an unfolded state without a definitive structure, but when a ligand peptide or partner protein coexists, the region interacts with it to form a complex by changing the random coil segments to secondary structures. It is suggested that disorder in a free state may actually be advantageous for the binding process, and that the rate of macromolecular association is enhanced by the presence of disorder region [36, 37]. As a way out of the situation, co-crystallization with some sort of ligands may work. That is, we should utilize the property of NUPs-like protein that is easy to change conformations by letting the protein change its structures, and by guiding it to a structure that is easier to be crystallized. The structural atlas of the protein promotes and deepens an understanding of the interaction between the complement proteins, which are involved in the human immune system, and drives novel drug development. Direct structural studies of the interaction between C4b and sCR1, or between C3b and sCR1 are desired to realize these goals [38].

4. Conclusions

Proteins like sCR1 are difficult targets to lead crystallization suitable for X-ray crystallography. The recognition of NUPs has imposed the view that proteins consist not only of structured domains but also of ID regions. The ID region is an unfolded state without a definitive structure, but when a ligand peptide or partner protein coexists, the region interacts with it

to form a complex by changing the random coil segments to rigid structured secondary structures. As a way out of the situation, co-crystallization with some sort of ligands or partner protein molecule may work. That is, we should utilize the flexible conformation property of NUPs-like protein, let the protein change its structures, and guide it to the structure that is easy to be crystallized. Once the structural detail of interest is obtained at hand, the atlas of the protein promotes and deepens the understanding of the interaction between the complement proteins which are involved in the immune system.

Acknowledgements

Conflict of interest

The author declares that he has any financial or personal relationships with people of organization that can inappropriately influence his work or the conclusions drawn from this investigation.

Author details

Noriyuki Ishii

Address all correspondence to: n.ishii@aist.go.jp

Biomedical Research Institute, Department of Life Science and Technology, National Institute of Advanced Industrial Science and Technology (AIST), Tsukuba, Ibaraki, Japan

References

[1] Anfinsen CB. Principles that govern the folding of protein chains. Science. 1973;**181**:223-230. DOI: 10.1126/science.181.4096.223

[2] Ellis RJ. Proteins as molecular chaperones. Nature. 1987;**328**:378-379. DOI: 10.1038/328378a0

[3] Akiba T, Ishii N, Rashid N, Morikawa M, Imanaka T, Harata K. Structure of RadB recombinase from a hyperthermophilic archaeon, *Thermococcus kodakaraensis* KOD1: An implication for the formation of a near-7-fold helical assembly. Nucleic Acids Research. 2005;**33**:3412-3423. DOI: 10.1093/nar/gki662

[4] Ishii N. Crystallization, structure and functional robustness of isocitrate dehydrogenases. In: Chandrasekaran A, editor. Current Trends in X-Ray Crystallography. Croatia: InTech; 2011. pp. 309-332. DOI: 10.5772/32635

[5] Dyson HJ, Wright PE. Intrinsically unstructured proteins and their functions. Nature Reviews Molecular Cell Biology. 2005;**6**:197-208. DOI: 10.1038/nrm1589

[6] Wright PE, Dyson HJ. Linking folding and binding. Current Opinion in Structural Biology. 2009;**19**:31-38. DOI: 10.1016/j.sbi.2008.12.003

[7] Wright PE, Dyson HJ. Intrinsically unstructured proteins: Re-assessing the protein structure-function paradigm. Journal of Molecular Biology. 1999;**293**:321-331. DOI: 10.1006/jmbi.1999.3110

[8] Nishikawa K. Natively unfolded proteins: An overview. Biophysics. 2009;**5**:53-58. DOI: 10.2142/biophysics.5.53

[9] Hoshino A, Costa-Silva B, Shen TL, Rodrigues G, Hashimoto A, Mark MT, Molina H, Kohsaka S, Di Giannatale A, Ceder S, Singh S, Williams C, Soplop N, Uryu K, Pharmer L, King T, Bojmar L, Davies AE, Ararso Y, Zhang T, Zhang H, Hernandez J, Weiss JM, Dumont-Cole VD, Kramer K, Wexler LH, Narendran A, Schwartz GK, Healey JH, Sandstrom P, Labori KJ, Kure EH, Grandgenett PM, Hollingsworth MA, de Sousa M, Kaur S, Jain M, Mallya K, Batra SK, Jarnagin WR, Brady MS, Fodstad O, Muller V, Pantel K, Minn AJ, Bissell MJ, Garcia BA, Kang Y, Rajasekhar VK, Ghajar CM, Matei I, Peinado H, Bromberg J, Lyden D. Tumour exosome integrins determine organotropic metastasis. Nature. 2015;**527**:329-335. DOI: 10.1038/nature15756

[10] Welton JL, Khanna S, Giles PJ, Brennan P, Brewis IA, Staffurth J, Mason MD, Clayton A. Proteomics analysis of bladder cancer exosomes. Molecular & Cell Proteomics. 2010; **9**:1324-1338. DOI: 10.1074/mcp.M000063-MCP201

[11] Melo SA, Luecke LB, Kahlert C, Fernandez AF, Gammon ST, Kaye J, LeBleu VS, Mittendorf EA, Weitz J, Rahbari N, Reissfelder C, Pilarsky C, Fraga MF, Piwnica-Worms D, Kalluri R. Glypican-1 identifies cancer exosomes and detects early pancreatic cancer. Nature. 2015;**523**:177-182. DOI: 10.1038/nature14581

[12] Ishii N, Fitrilawati F, Manna A, Akiyama H, Tamada Y, Tamada K. Gold nanoparticles used as a carrier enhance production of anti-hapten IgG in rabbit: A study with azobenzene-dye as a hapten presented on the entire surface of gold nanoparticles. Bioscience, Biotechnology, and Biochemistry. 2008;**72**:124-131. DOI: 10.1271/bbb.70499

[13] Nelson RA Jr. The immune adherence phenomenon. Science. 1953;**118**:733-737. DOI: 10.1126/science.118.3077.733

[14] Nelson DS. Immune adherence. In: Dixon DS, Humphrey JH Jr, editors. Advances in Immunology. Vol. 3. New York: Academic Press Inc.; 1963. pp. 131-180

[15] Fearon DT. Regulation of the amplification C3 convertase of human complement by an inhibitory protein isolated from human erythrocyte membrane. Proceedings of the National Academy of Sciences of the United States of America. 1979;**76**:5867-5871. PMCID: PMC411753

[16] Fearon DT. Identification of the membrane glycoprotein that is the C3b receptor of human erythrocyte, polymorphonuclear leukocyte, B lymphocyte, and monocyte. The Journal of Experimental Medicine. 1980;**152**:20-30. PMCID: PMC2185895

[17] Krych-Goldberg M, Atkinson JP. Structure-function relationship of complement receptor type 1. Immunological Reviews. 2001;**180**:112-122. DOI: 10.1034/j.1600-065X.2001.1800110.x

[18] Weisman HF, Bartow T, Leppo MK, Marsh HC Jr, Carson GR, Concino MF, Boyle MP, Roux KH, Weisfeldt ML, Fearon DT. Soluble human complement receptor type 1: In vivo inhibitor of complement suppressing post-ischemic myocardial inflammation and necrosis. Science. 1990;**249**:146-151. DOI: 10.1126/science.2371562

[19] Kato H, Inoue T, Ishii N, Murakami Y, Matsumura M, Wang PC. A novel simple method to purify recombinant soluble human complement receptor type 1 (sCR1) from CHO cell culture. Biotechnology and Bioprocess Engineering. 2002;**7**:67-75. DOI: 10.1007/BF02935882

[20] Yamaguchi A, Takagawa H, Iwakaji H, Miyagawa S, Wang PC, Ishii N. Construction of the plasmid, expression by Chinese hamster ovary cell, purification and characterization of the first three short consensus repeat modules of human complement receptor type 1. Journal of Biochemistry. 2009;**145**:533-542. DOI: 10.1093/jb/mvp006

[21] Ishii N, Kato H, Wang PC. Observation by electron microscopy on recombinant soluble human complement receptor type 1 (sCR1) and its derivative, aglyco-sCR1, from CHO cells. Enzyme and Microbial Technology. 2003;**33**:482-487. DOI: 10.1016/S0141-0229(03)00152-2

[22] Mevorach D, Mascarenhas JO, Gershov D, Elkon KB. Complement-dependent clearance of apoptotic cells by human macrophages. Journal of Experimental Medicine. 1998;**188**:2313-2320. DOI: 10.1084/jem.188.12.2313

[23] Carrington CA, dos Santos Cruz G. Effect of cell surface concentration of human DAF on transgenic pig aortic endothelial cells on the degree of protection afforded against human complement deposition. Xenotransplantation. 2001;**8**:100-105. DOI: 10.1034/j.1399-3089.2001.00086.x

[24] Huang J, Gou D, Zhen C, Jiang D, Mao X, Li W, Chen S, Cai C. Protection of xenogeneic cells from human complement-mediated lysis by the expression of human DAF, CD59 and MCP. FEMS Immunology and Medical Microbiology. 2001;**31**:203-209. DOI: 10.1111/j.1574-695X.2001.tb00521.x

[25] Ishii N, Umemura K, Miyazaki K. Supramolecular complex formation and crystallization of isocitrate dehydrogenase from *Thermus thermophilus* HB8: Preliminary studies with X-ray crystallography and atomic force microscopy. Bioscience, Biotechnology, and Biochemistry. 2008;**72**:2369-2376. DOI: 10.1271/bbb.80269

[26] Nishikawa K, Noguchi T. Predicting protein secondary structure based on amino acid sequence. Methods in Enzymology. 1991;**202**:31-44. DOI: 10.1016/0076-6879(91)02005-T

[27] Ito M, Matsuo Y, Nishikawa K. Prediction of protein secondary structure using the 3D-1D compatibility algorithm. Computer Applications in the Biosciences. 1997;**13**:415-424

[28] Klickstein LB, Barbashov SF, Liu T, Jack RM, Nicholson-Weller A. Complement receptor type 1 (CR1, CD35) is a receptor for C1q. Immunity. 1997;**7**:345-355. DOI: 10.1016/S1074-7613(00)80356-8

[29] Makrides SC, Scesney SM, Ford PJ, Evans KS, Carson GR, Marsh HC Jr. Cell surface expression of the C3b/C4b receptor (CR1) protects Chinese hamster ovary cells from lysis by human complement. Journal of Biological Chemistry. 1992;**267**:24754-24761

[30] Reilly BD, Makrides SC, Ford PJ, Marsh HC Jr, Mold C. Quantitative analysis of C4b dimer binding to distinct sites on the C3b/C4b receptor (CRl). Journal of Biological Chemistry. 1994;**269**:7696-7701

[31] Wong WW, Farrell SA. Proposed structure of the F' allotype of human CR1. Loss of a C3b binding site may be associated with altered function. Journal of Immunology. 1991;**146**:656-662

[32] Reilly BD, Mold C. Quantitative analysis of C4Ab and C4Bb binding to the C3b/C4b receptor (CR1, CD35). Clinical and Experimental Immunology. 1997;**110**:310-316. DOI: 10.1111/j.1365-2249.1997.tb08333.x

[33] Ishii N, Saijo S, Sato T, Tanaka N, Harata K. Crystallization and preliminary X-ray studies of V_1-ATPase of *Thermus thermophilus* HB8 complexed with Mg-ADP. Journal of Structural Biology. 2001;**134**:88-92. DOI: 10.1006/jsbi.2001.4358

[34] Furtado PB, Huang CY, Ihyembe D, Hammond RA, Marsh HC, Perkins SJ. The partly folded back solution structure arrangement of the 30 SCR domains in human complement receptor type 1 (CR1) permits access to its C3b and C4b ligands. Journal of Molecular Biology. 2008;**375**:102-118. DOI: 10.1016/j.jmb.2007.09.085

[35] Smith BO, Mallin RL, Krych-Goldberg M, Wang X, Hauhart RE, Bromek K, Uhrin D, Atkinson JP, Barlow PN. Structure of the C3b binding site of CR1 (CD35), the immune adherence receptor. Cell. 2002;**108**:769-780. DOI: 10.1016/S0092-8674(02)00672-4

[36] Shoemaker BA, Portman JJ, Wolynes PG. Speeding molecular recognition by using the folding funnel: The fly-casting mechanism. Proceedings of the National Academy of Sciences of the United States of America. 2000;**97**:8868-8873. DOI: 10.1073/pnas.160259697

[37] Pontius BW. Close encounters: why unstructured, polymeric domains can increase rates of specific macromolecular association. Trends in Biochemical Sciences. 1993;**18**:181-186. DOI: 10.1016/0968-0004(93)90111-Y

[38] Ishii N, Sato T. Anisotropic intersubunit and inter-ring interactions revealed in the native bullet-shaped chaperonin complex from *Thermus thermophilus*. Biochimica et Biophysica Acta. 1830;**2013**:2907-2916. DOI: 10.1016/j.bbagen.2013.01.003